Two-magnon excitations in the Heisenberg ferromagnet with uniaxial anisotropy

A. A. Bahurmuz and P. D. Loly

Department of Physics, University of Manitoba, Winnipeg, Manitoba R3T 2N2 Canada

(Received 29 October 1979)

Two-magnon excitations are examined in detail for the nearest-neighbor simple-cubic Heisenberg ferromagnet with various values of uniaxial anisotropy and all total wave vectors ($\vec{K}$) in the [111] direction. Attention is focused on the changes brought about by the addition of a single-ion-pair mode to the basic exchange-pair modes of the isotropic case. The propagator for exchange pairs separates into a contribution from the d-wave mode and a combined effect from s-wave exchange and single-ion pairings. The latter has the same denominator as the propagator for single-ion pairs but exhibits very little of the strong single-ion resonance due to the vanishing of the numerator at the position of the single-ion Ising level. Lattice Green's functions approaching analytic quality have been used to evaluate various spectral components in order to establish how the single-ion mode behaves in the two-magnon continuum. For values of uniaxial anisotropy such that the single-ion Ising level crosses the s-wave bound-state mode of the isotropic case, we find that the single-ion resonance correlates well with the corresponding Ising level in the continuum but evolves continuously to the s-wave exchange bound state at the zone boundary.

I. INTRODUCTION

Two-magnon bound states occur in the Heisenberg ferromagnet with nearest-neighbor (NN) interactions for large total pair wave vector $\vec{K}$.[1-6] As $\vec{K}$ decreases, Boyd and Callaway[3] have shown that some of the bound states enter the two-magnon continuum as resonances. Silberglitt and Harris[7] examined the effect of two-magnon bound states and resonances on the one-magnon propagator at finite temperatures while Loly and Choudhury[8] investigated the bound-state-resonance mode for all $\vec{K}$. Two-magnon studies have been extended to include anisotropic exchange,[1,8-10] uniaxial anisotropy,[9-15] biquadratic exchange,[10,12,15,16] and next-nearest-neighbor (NNN) interactions.[17-19]

In the NN simple-cubic Heisenberg ferromagnet with $\vec{K}$ in the [111] direction, nondegenerate s-wave and doubly degenerate d-wave exchange bound states are formed for large $\vec{K}$.[1,3] As $\vec{K}$ decreases, the d-wave bound states enter the continuum as resonances[3] while the s wave joins in a grazing fashion. In the presence of uniaxial anisotropy [with single-ion energy $-D(S_i^z)^2$] an additional single-ion bound state is found[9-15] which interacts with the original s-wave bound state. There was an early indication[14] of a difference in the behavior of the single-ion and d-wave resonances, but the resolution of the spectral functions at that time was limited by the accuracy of the lattice Green's functions (LGF) employed. In this paper we complement the single-ion bound-state study of Silberglitt and Torrance[11] for $D \neq 0$ by a thorough study of the two-magnon continuum resonances and their relationship to bound states which is

made possible by the use of accurate LGF's obtained from elliptic integrals.[20] The relative positions of the single-ion and exchange bound states depend on the ratio D/J (where J is the exchange constant) and fall into three distinct regions recognized already in the work of Silberglitt and Torrance.[11] For the middle region, when the single-ion Ising level crosses the s-wave mode of the isotropic case, the interaction of the single-ion and s-wave bound-state modes will be shown to give a strong effect on the resonance-bound-state evolution. A comparative analysis of both single-ion and exchange-pairing cross sections leads to a full understanding of the differences between those spectra.

Section II gives an outline of the derivation of the Dyson equation for the two-magnon propagators at $T = 0$ K for a Heisenberg ferromagnet with single-ion anisotropy. The solutions for single-ion and NN processes are given in Sec. III. In Sec. IV the results of numerical computations for bound states and resonances are discussed and the conclusions are given in Sec. V.

II. TWO-MAGNON PROPAGATOR

The Heisenberg Hamiltonian in the presence of uniaxial anisotropy has the form

$$H = -\sum_{ij} J_{ij} \vec{S}_i \cdot \vec{S}_j - \sum_i D(S_i^z)^2 , \qquad (1)$$

where J_{ij} is the exchange constant between spins at sites i and j, and D is the uniaxial anisotropy. The Green's function describing the scattering of two

magnons with initial wave vectors $\vec{k}_1'$, $\vec{k}_2'$ and final wave vectors $\vec{k}_1$, $\vec{k}_2$ is

$$G(\vec{k}_1\vec{k}_2, \vec{k}_1'\vec{k}_2', t) = -i\Theta(t)\langle 0|[S_{\vec{k}_1}^-(t)S_{\vec{k}_2}^-(t), S_{\vec{k}_1'}^+(0)S_{\vec{k}_2'}^+(0)]|0\rangle = \langle\langle S_{\vec{k}_1}^-(t)S_{\vec{k}_2}^-(t)|S_{\vec{k}_1'}^+(0)S_{\vec{k}_2'}^+(0)\rangle\rangle \quad , \quad (2)$$

where $S_{\vec{k}}^\alpha$ is the Fourier transform of S_i^α and $|0\rangle$ is the fully aligned ground state defined such that $S_i^z|0\rangle = -S|0\rangle$ and $S_i^-|0\rangle = 0$. The equation of motion for the Green's function in Eq. (2) has the standard form

$$\omega G(\vec{K}\vec{k}, \vec{K}'\vec{k}', \omega) = \langle 0|[S_{\vec{k}_1}^- S_{\vec{k}_2}^-, S_{\vec{k}_1'}^+ S_{\vec{k}_2'}^+]|0\rangle + \langle\langle [S_{\vec{k}_1}^-(t)S_{\vec{k}_2}^-(t), H]|S_{\vec{k}_1'}^+(0)S_{\vec{k}_2'}^+(0)\rangle\rangle_\omega \quad , \quad (3)$$

where $G(..., \omega)$ and $\langle\langle \cdots \rangle\rangle_\omega$ are Fourier transforms and where the total and relative pair wave vectors are defined by

$$\vec{K} = \vec{k}_1 + \vec{k}_2 \quad , \quad 2\vec{k} = \vec{k}_1 - \vec{k}_2 \quad , \quad \vec{K}' = \vec{k}_1' + \vec{k}_2' \quad , \quad 2\vec{k}' = \vec{k}_1' - \vec{k}_2' \quad . \quad (4)$$

We now introduce the partial Fourier transform

$$G(ij, \vec{K}, \omega) = \frac{1}{N}\sum_{\vec{k}\vec{k}'} e^{-i\vec{k}\cdot\vec{R}_i}e^{i\vec{k}'\cdot\vec{R}_j}G(\vec{K}\vec{k}, \vec{K}\vec{k}', \omega) \quad . \quad (5)$$

The Dyson equation for the above propagator is[19]

$$G(ij, \vec{K}, \omega) = 8S^2\left[1 - \frac{\delta_{j0}}{2S}\right]\Lambda(ij, \vec{K}, \omega) + 2\sum_l J_l\tilde{\Lambda}(il, \vec{K}, \omega)G(lj, \vec{K}, \omega) - 2\sum_l D\Lambda(il, \vec{K}, \omega)G(lj, \vec{K}, \omega)\delta_{l0} \quad , \quad (6)$$

where

$$\Lambda(ij, \vec{K}, \omega) = \frac{1}{N}\sum_{\vec{k}}\frac{\cos\vec{k}\cdot\vec{R}_i\cos\vec{k}\cdot\vec{R}_j}{\omega - \Omega(\vec{K}, \vec{k})} \quad , \quad (7)$$

$$\tilde{\Lambda}(ij, \vec{K}, \omega) = \frac{1}{N}\sum_{\vec{k}}\frac{\cos\vec{k}\cdot\vec{R}_i(\cos\frac{1}{2}\vec{K}\cdot\vec{R}_j - \cos\vec{k}\cdot\vec{R}_j)}{\omega - \Omega(\vec{K}, \vec{k})} \quad (8)$$

and Ω is the two-magnon dispersion function given by

$$\Omega(\vec{K}, \vec{k}) = 2S[2J(0) - J(\tfrac{1}{2}\vec{K} + \vec{k}) - J(\tfrac{1}{2}\vec{K} - \vec{k})] + 2(2S - 1)D \quad . \quad (9)$$

For $D = 0$ the Dyson equation in Eq. (6) reduces to that given by Wortis.[1] The solution to Eq. (6) will be discussed in the next section. We note here that the functions Λ and $\tilde{\Lambda}$ that appear in this equation are expressible in terms of the LGF which for site i are defined as

$$L_i(\omega) = \frac{1}{N}\sum_{\vec{k}}\frac{e^{i\vec{k}\cdot\vec{R}_i}}{\omega - \Omega(\vec{K}, \vec{k})} \quad . \quad (10)$$

III. TWO-MAGNON SPECTRA

The Green's function $G(ii, \vec{K}, \omega)$ in Eq. (6) represents the propagator for two-magnon processes involving the creation of two spin deviations on sites separated by a distance $\vec{R}_i$. The spectral functions for such processes are given by $X_{ii}(\vec{K}, \omega) = -\text{Im}\,G \times (ii, \vec{K}, \omega)$. In this paper we examine processes involving the creation of two spin deviations on the same site $[\vec{R}_0 = (0, 0, 0)]$ and NN sites $[\vec{R}_1 = (1, 0, 0)a]$. In shorthand notation these sites are denoted by $i = 0$ and 1, respectively. We note here that for $\vec{K} = 0$, Thorpe[21] has shown that $X_{00}(0, \omega)$ is proportional to the cross section for two-magnon Raman scattering through the spin-orbit interaction in ferromagnets, while the best analog of the exchange process responsible for the antiferromagnetic observations is given by X_{11} [which was studied earlier for the isotropic NN simple cubic (sc) case[8]].

For the NN sc problem with $\vec{K}$ in the [111] direction, we find the following solutions to Eq. (6):

$$\hat{G}(00, \vec{K}, \omega) = 48S^2\left[1 - \frac{1}{2S}\right]\frac{Z}{(X + dZ)} \quad , \quad (11)$$

$$\hat{G}(11,\vec{K},\omega) = \frac{4S^2}{3}\left\{\frac{\left[1+\frac{1}{6}dl_{000}\right](L_{000}+L_{200}+4L_{110}) - dL_{100}^2}{(X+dZ)} + \frac{2(L_{000}+L_{200}-2L_{110})}{Y}\right\} , \qquad (12)$$

in which $G = \hat{G}/24SJ$, $d = D/2SJ$, and where

$$Z = \frac{1}{6}\left\{XL_{000} + \frac{L_{100}(\alpha L_{000} - L_{100})}{2S}\right\} , \qquad (13)$$

$$X = 1 - \frac{\alpha L_{100}}{2S} + \frac{(L_{000}+L_{200}+4L_{110})}{12S} , \qquad (14)$$

$$Y = 1 + \frac{(L_{000}+L_{200}-2L_{110})}{12S} . \qquad (15)$$

In the above, $\alpha = \cos(\frac{1}{2}K_x a)$ and L_{lmn} are normalized LGF's for $\vec{R}_i = (l,m,n)a$ which can be written as

$$L_{lmn}(\hat{\omega}) = \frac{1}{\pi^3}\int\int\int_0^\pi \frac{\cos lx \cos my \cos nz}{\hat{\omega}-\hat{\Omega}}dx\,dy\,dz , \qquad (16)$$

where $x = k_x a$, etc., and where we have introduced the normalized energies

$$\hat{\omega} = [\omega - 2(2S-1)D]/24SJ , \qquad (17)$$

$$\hat{\Omega} = [\Omega - 2(2S-1)D]/24SJ$$
$$= 1 - \frac{1}{3}\alpha(\cos x + \cos y + \cos z) . \qquad (18)$$

In Eqs. (17) and (18) $24SJ$ is the one-magnon

bandwidth and $2(2S-1)D$ eliminates the constant shift due to the gap in the one-magnon spectrum. The five LGF's appearing in Eqs. (11)–(15) are not all independent, and we have the following identities:

$$1 = (\hat{\omega}-1)L_{000} + \alpha L_{100} ; \qquad (19)$$

$$0 = (\hat{\omega}-1)L_{100} + \frac{1}{6}\alpha(L_{000}+L_{200}+4L_{110}) . \qquad (20)$$

We use Eqs. (19) and (20) to eliminate L_{100} and L_{110} and the remaining LGF's are evaluated in terms of elliptic integrals using the method of Horiguchi and Morita.[20] The relationship between $L_{lmn}(\hat{\omega})$ and the LGF's $G_{lmn}(t)$ defined by these authors is

$$L_{lmn}(\hat{\omega}) = -(3/\alpha)G_{lmn}(3(1-\hat{\omega})/\alpha) . \qquad (21)$$

IV. RESULTS

Before we examine two-magnon bound states and resonances it is necessary to briefly discuss critical points[22] and Ising levels.[23] The two-magnon continuum is given by Eq. (18) with a relevant portion exhibited in Fig. 1. The critical points are defined as

(a) $1-\alpha$ (b) $1-\alpha$ (c) $1-\alpha$
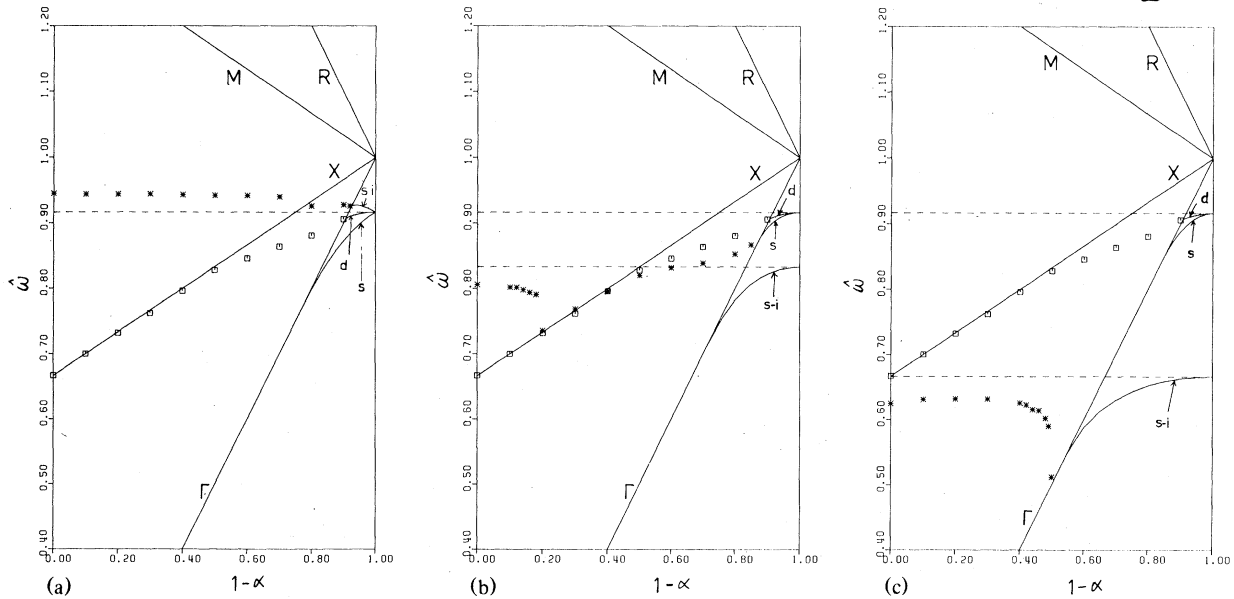
FIG. 1. Dispersion of resonance peaks and bound states as a function of $\vec{K}$ for $S = 1$ and (a) $d = 0.5$, (b) $d = 1.0$, and (c) $d = 2.0$. The full straight lines correspond to the critical points Γ, X, M, and R where Γ and R represent the bottom and top of the two-magnon continuum, respectively. The horizontal broken lines are the Ising levels for single-ion ($\hat{\omega} = 1 - \frac{1}{6}d$) and nearest-neighbor ($\hat{\omega} = 1 - 1/12S$) excitations. The single-ion, s- and d-wave exchange bound states are indicated by $s-i$, s, and d, respectively, while * and □ represent the single-ion and d-wave resonances, respectively.

those points in $\vec{k}$ space where the group velocity of the two-magnon dispersion function vanishes. For the NN sc problem the critical points are given by the high-symmetry points $\Gamma = (0,0,0)$, $X = (1,0,0)\pi/a$, $M = (1,1,0,)\pi/a$, and $R = (1,1,1)\pi/a$, and the two-magnon energies at these points are indicated by the straight lines in Fig. 1.[8,24] The Ising levels are obtained by neglecting the transverse terms in the exchange part of the Hamiltonian in Eq. (1). The energy required to create two spin deviations on neighboring sites in this limit is $4SJ(0) + 2(2S-1)D - 2J$, while two deviations on the same site require an energy $4SJ(0) + 2(2S-1)D - 2D$,[23] and these are both shown by the horizontal broken lines in Fig. 1.

The two-magnon bound states are given by the poles of the propagator in Eqs. (11) and (12). Thus the bound-state conditions are

$$X + dZ = 0 \ , \tag{22}$$

$$Y = 0 \ . \tag{23}$$

These were first obtained by Wortis[1] for the isotropic $(D=0)$ case and by Silberglitt and Torrance[11] and Tonegawa[9] for $D \neq 0$ and are the same as those given by Loly and Choudhury.[8] For $D=0$, Eqs. (22) and (23) give the s- and d-wave exchange bound states, respectively. The d-wave bound state is unaf-

fected by the uniaxial anisotropy, while for $D \neq 0$, Eq. (22) leads to a modified s-wave exchange bound state and an additional single-ion bound state.[11] At the Brillouin-zone (BZ) corner

$$(\alpha = 0), \quad L_{lmn}(\hat{\omega}) = \delta_{l0}\delta_{m0}\delta_{n0}(\hat{\omega}-1)^{-1}$$

and it is then trivial to solve Eqs. (22) and (23). The result is that the s- and d-wave bound states are degenerate at $\hat{\omega} = 1 - 1/12S$, while the single-ion one occurs at $\hat{\omega} = 1 - d/6$. These energies correspond to the Ising levels for NN and single-ion excitations, respectively, as discussed above. Away from the BZ corner, the bound-state energies are obtained by a numerical solution of Eqs. (22) and (23). As α increases, the bound states approach the bottom of the continuum. The points of contact are given by substituting for $\hat{\omega}$ the energy of the bottom of the band in Eqs. (22) and (23), viz., $1 - \alpha$. From Eq. (23), we find that the d wave enters the continuum at

$$\alpha = \{2 + 3[G_{200}(3) - G_{000}(3)]\}/8S \approx 0.0926/S \ .$$

This result was first obtained by Wortis.[1] On the other hand, Eq. (22) gives a quadratic equation in α

$$A\alpha^2 + B\alpha + C = 0 \ , \tag{24a}$$

(a)

(b)
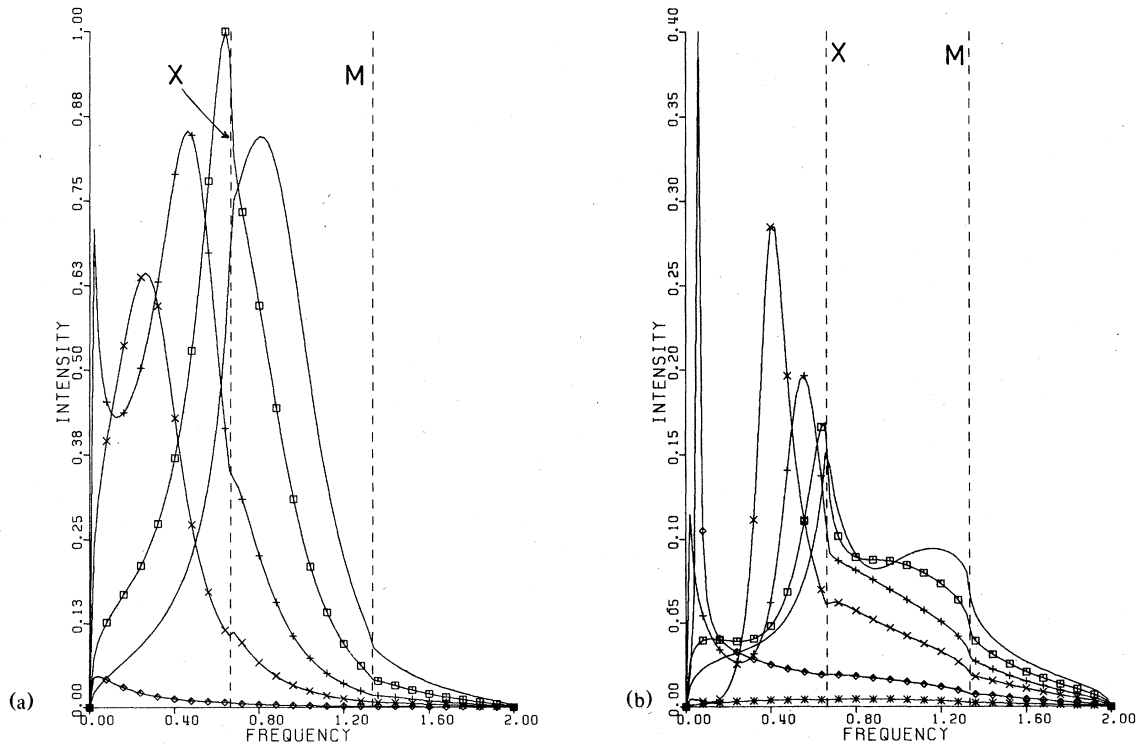
FIG. 2. Spectra for (a) single-ion (X_{00}) and (b) NN (X_{11}) excitations for selected values of $\vec{K}$ for $S=1$ and $d=1.0$. The curves represent $\alpha = 1.0$ (full line), 0.5 ($\square$), 0.3 (+), 0.2 ($\times$), 0.1 ($\diamond$), and 0.05 (*). For clarity the relative intensities were multiplied by α and the frequency scaled to a bandwidth of 2.0. For (b), the $\alpha = 0.1(\diamond)$ spectra extends to 1.0 but has been cut off at 0.4 for convenience. The vertical broken lines represent the X and M critical points.

where

$$A = 2(W - 1 + 2S) , \qquad (24b)$$

$$B = 2[1 - (1 + Sd/3) W] , \qquad (24c)$$

$$C = \frac{1}{3} d (W - 1) , \qquad (24d)$$

where $W = 3G_{000}(3) = 1.516386$ is the Watson integral. The two solutions of the above equation correspond to the points where the other two bound states meet the continuum. We note that for $d = 0$, the nonzero solution of Eq. (24a) is $\alpha = -B/A$ $\approx (1 + 4S/1.03277)^{-1}$ which is also consistent with Wortis.[1] For $S = 1$, this s-wave contact point is ≈ 0.205 and corresponds to a single-ion Ising level with $d \approx 1.23$. In the presence of uniaxial anisotropy, the two solutions of Eq. (24) are 0.232 and 0.074 for $d = 0.5$, 0.287 and 0.119 for $d = 1.0$, and 0.457 and 0.150 for $d = 2.0$.

The dispersions of the bound states for $d = 0.5$, 1.0, and 2.0 are shown in Fig. 1. We note that the d-wave variety does not appear in $G(00, \vec{K}, \omega)$. For $d = 0.5$ all the bound states are degenerate at the zone boundary, and we see repulsion between the s wave and single-ion states for smaller $\vec{K}$. The case of $d = 1.0$ represents the intermediate cross-over region where the single-ion Ising level crosses the s-wave mode of the isotropic case. The case of $d = 2.0$ is chosen to illustrate the situation on the other side of the cross-over region and has a single-ion Ising level equal to the minimum of the X-point singularity. Note the dispersion of the lowest bound state in Fig. 1(c) associated with the lower edge of the continuum.

The spectral functions for selected values of $\vec{K}$ and for $d = 1.0$ are shown in Fig. 2 to illustrate the basis for resonance peaks plotted in Fig. 1. The single-ion (X_{00}) spectrum in Fig. 2(a) is characterized by one well-defined resonance peak for most values of $\vec{K}$ and an additional spike in the neighborhood of $\alpha = 0.3$. As $\vec{K}$ increases, the principal peak moves towards the lower edge of the continuum until finally it exists from the continuum as a discrete bound state [as seen in Fig. 1(b)]. The additional sharp lower peak near the bottom of the band seen for $\alpha = 0.3$ indicates a pickup of weight due to the bound state which has just joined the continuum at $\alpha \approx 0.287$. In contrast the NN (X_{11}) spectrum in Fig. 2(b) has another well-defined resonance peak with pronounced wings which result in a very broad hump on the upper side at small values of $\vec{K}$. The well-defined lower peak is due to the d-wave exchange resonance, but the hump is not as easy to interpret. Some handle on this spectrum is afforded by examining separately the two components of Eq. (12). The first term has the same denominator as the single-ion probe in Eq. (11) so that it embodies the s-wave exchange and single-ion modes, and we have seen that the second term is responsible for the d-wave effect

which is not found in X_{00}. Figure 3 shows a sample case of these separate components of X_{11} and their sum from which we note the vanishing of the first term at an energy close to the peak in X_{00}. Rearrangement of the numerator of the non-d-wave part of $G(11, \vec{K}, \omega)$ using the LGF identities in Eqs. (19) and (20) shows that this numerator vanishes identically at the single-ion Ising level. We therefore see the product of a resonance structure and a term which zeros near its peak to yield broad humps on either side that represent a partitioning of the single-ion effect. Again the additional sharp lower peak near the bottom of the band for $\alpha = 0.3$ is due to the bound state which joined the continuum at $\alpha \approx 0.287$. For the NN spectrum the d-wave bound state enters the continuum for $\alpha \approx 0.0926$ and hence a resonance peak can still be seen for $\alpha = 0.1$ while for $\alpha = 0.05$ the resonance has come out of the continuum as a discrete bound state leaving a very weak broad spectrum inside the band as shown.

The dispersion of the resonance-peak positions as a function of $\vec{K}$ is shown in Fig. 1 for three values of d. We note that the d-wave resonance is always constrained below the X critical point and is independent of the uniaxial anisotropy. In contrast the single-ion type of resonance (for $d = 0.5$ and 1.0) is able to go
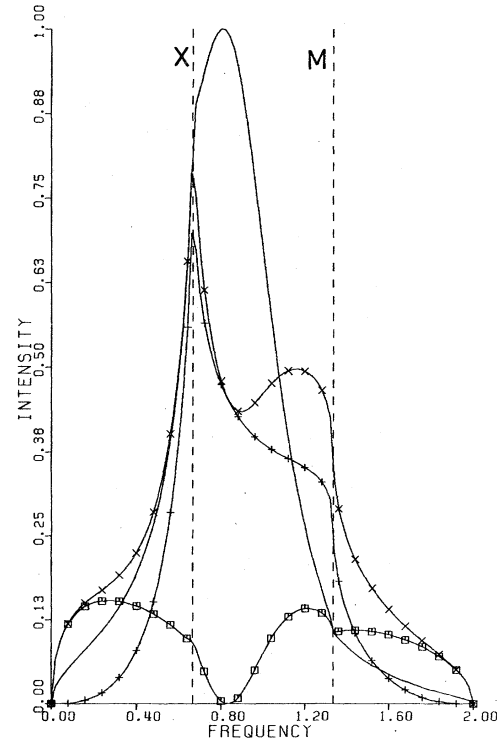
FIG. 3. Components of the NN spectra for $\vec{K} = 0$, $S = 1$, and $d = 1.0$. □ and + represent the first and second terms of $G(11, \vec{K}, \omega)$ [Eq. (12)], respectively, and × gives their sum. The full line is the single-ion $[G(00, \vec{K}, \omega)]$ spectrum.

through that singularity, and approaches the corresponding Ising level at the zone center. The crossover case of $d = 1.0$ shows a strong single-ion resonance in $X_{00}(\vec{K}, \omega)$ which stays close to the Ising level from $\vec{K} = 0$, during its passage through the X-point singularity, until it exists as a bound state. The latter then evolves to reach the zone boundary as the s-wave exchange bound state. For $d = 2.0$, Fig. 2(c) shows how the single-ion bound state jumps into the continuum in a manner rather different from the smooth transition of the d-wave mode.

The behavior of resonances just inside the continuum was detected in some cases by Silberglitt and Torrance[11] through the analysis of zeros of the bound-state conditions [Eqs. (22) and (23)] inside the continuum. Since resonance structures evolve continuously as they get deeper into the continuum we have been able to follow the resonances all the way to $\vec{K} = 0$ through the peaks of the resonant components of the spectra.

V. CONCLUSIONS

In this paper we have examined the behavior of two-magnon states in the NN sc Heisenberg ferromagnet with uniaxial anisotropy. The dispersion of the two-magnon bound states and resonances was examined in detail for all total pair wave vectors $\vec{K}$ in the [111] direction. For intermediate values of d, a crossover of the single-ion Ising level and the s-wave mode of the isotropic case occurs with a dramatic change of character between the single-ion Raman resonance at $\vec{K} = 0$ and its continuous evolution to the s-wave exchange bound state at the zone boundary. Within the continuum the single-ion resonance goes through the X critical point in contrast to the d-wave resonance which is constrained below it. Our results also show that the single-ion resonance at the zone center is always close to the corresponding Ising level for single-site excitations, although it may be depressed by the continuum for d in the range approximately 1.23 to 4.9. Finally, the ingredients of the spectra for the single-ion and exchange probes have been elucidated and reveal that the strongest single-ion Ising-level effect gives a spectral contribution that is perhaps best described as the antithesis of a resonance.

ACKNOWLEDGMENT

[1]M. Wortis, Phys. Rev. 132, 85 (1963).

[2]J. Hanus, Phys. Rev. Lett. 11, 336 (1963).

[3]R. G. Boyd and J. Callaway, Phys. Rev. 138, A1621 (1965).

[4]A. M. Bonnot and J. Hanus, Phys. Rev. B 7, 2207 (1973).

[5]A. W. Saenz and W. W. Zachary, J. Math. Phys. (N.Y.) 14, 1837 (1973).

[6]K. Wada and Y. Mizuta, Phys. Lett. A 59, 311 (1976).

[7]R. Silberglitt and A. B. Harris, Phys. Rev. Lett. 19, 30 (1967); Phys. Rev. 174, 640 (1968).

[8]P. D. Loly and B. J. Choudhury, Phys. Rev. B 13, 4019 (1976).

[9]T. Tonegawa, Prog. Theor. Phys. Suppl. 46, 61 (1970).

[10]D. A. Pink and R. Ballard, Can. J. Phys. 52, 33 (1974).

[11]R. Silberglitt and J. B. Torrance, Phys. Rev. B 2, 772 (1970).

[12]D. A. Pink and P. Tremblay, Can. J. Phys. 50, 1728 (1972).

[13]B. J. Choudhury and P. D. Loly, in Proceedings of the 20th Conference on Magnetism and Magnetic Materials, San

Francisco, 1974, edited by C. D. Graham, Jr., G. H. Lander, and J. J. Rhyne, AIP Conf. Proc. No. 24 (AIP, New York, 1975).

[14]P. D. Loly, in Proceedings of the Third International Conference on Light Scattering in Solids, edited by M. Balkanski (Flammarion, Paris, 1976), p. 274.

[15]S. T. Chiu-Tsao, Phys. Rev. B 13, 3175 (1976).

[16]S. T. Chiu-Tsao, P. M. Levy, and C. Paulson, Phys. Rev. B 12, 1819 (1975).

[17]P. D. Loly, B. J. Choudhury, and W. R. Fehlner, Phys. Rev. B 11, 1996 (1975).

[18]S. Krompiewski, Acta Phys. Pol. A 53, 845 (1978).

[19]A. A. Bahurmuz and P. D. Loly, Phys. Rev. B (in press).

[20]T. Horiguchi and T. Morita, J. Phys. C 8, L232 (1975).

[21]M. F. Thorpe, Phys. Rev. B 4, 1608 (1971).

[22]L. Van Hove, Phys. Rev. 89, 1189 (1953).

[23]R. J. Elliott and A. J. Smith, J. Phys. (Paris) 32, C1-585 (1971).

[24]A. A. Bahurmuz and P. D. Loly, Phys. Rev. B 19, 5803 (1979).